MODELING OF LARGE APERTURE TRANSDUCER FOCUSING IN CYLINDRICAL BILLETS

R. A. Roberts
Center for NDE
Iowa State University
Ames, IA 50012

INTRODUCTION

This paper presents the application of beam transmission modeling to the problem of large aperture transducer focusing in cylindrical billets. This work is to aid in the design and procurement of large aperture bi-cylindrically focused transducers for use in the multi-zone billet inspection system being developed under the FAA Engine Titanium Consortium (ETC) program. Need for this work arises from 1) errors due to diffraction and focusing aberrations which occur when established optical lens formulas are employed in the design of acoustic lenses, 2) focusing errors resulting from billet surface geometric irregularities which are not readily handled by other beam model approaches.

The approach taken in this work is to express the beam transmitted into the billet in an integral representation involving the Green function for the water/billet system. The Green function is evaluated asymptotically by ray theory. The integral representation is then evaluated numerically using an efficient quadrature which rigorously accounts for aperture diffraction. The incident beam to be transmitted into the billet is generated in experiments by a bi-cylindrically focused fixed lens/piezoelectric element system. A simple ray model is employed to obtain an equivalent pressure field in water which propagates in like fashion to that generated by the lens/element system, which is then used in the numerical evaluation of the field representation integral.

In the following, the solution approach is outlined and numerical results are presented for cases of interest. The effects of aperture size on focal zone depth and geometry are demonstrated. Also, the sensitivity of the focal zone geometry to irregularities in the billet surface profile is studied. Comparisons are made to the Gauss-Hermite beam model employed in related modeling work within the ETC program, which demonstrates the validity and limitations of the Gauss-Hermite polynomial expansion.

BEAM TRANSMISSION AND TRANSDUCER/LENS MODELS

The problem geometry is depicted in fig.1. A reference plane P is positioned in the water exterior to the billet. In the absence of the billet, a time-harmonic incident beam is represented forward of the reference plane (in the direction of the billet) by the Fourier transform

$$p(x) = \int \hat{p}(\underline{k})\, exp(i\, k_3\, x_3)\, exp(i\, k_1\, x_1 + i\, k_2\, x_2)\, d\underline{k} \qquad (1)$$

Review of Progress in Quantitative Nondestructive Evaluation, Vol. 14
Edited by D.O. Thompson and D.E. Chimenti, Plenum Press, New York, 1995

where coordinates x_j , j=1,2,3 , are defined such that the reference plane is x_3=0. The two-dimensional Fourier transform variable vector $\underline{k}$ =(k_1, k_2) corresponds to transformation in $\underline{x}$ = (x_1, x_2). The wave vector component k_3 is given by

$$k_3 = (k_w^2 - k_1^2 - k_2^2)^{1/2}, \quad k_w = \omega / c_w \tag{2}$$

where ω is time harmonic frequency, c_w is the wavespeed in water, and the root is defined to insure wavefield propagation or decay in the $+x_3$ direction. The quantity $\hat{p}$ denotes the Fourier transform of p(x) in the x_1, x_2 reference coordinates with x_3=0. Noting that eq.(1) is the Fourier transform of the product of two factors, the convolution theorem yields

$$p(x') = \int_{x_3=0} p(x)\, G(x' - x)\, d\underline{x} \tag{3}$$

where the quantity

$$G(x' - x) = C \frac{x_3}{r^2} \left(1 - \frac{1}{ik_w r}\right) exp(ik_w r), \quad r = |x' - x|, \quad x_3' > x_3 \tag{4}$$

is recognized (to within a multiplicative constant C) as the x_3 derivative of the Green function for an infinite fluid medium. The x_3 derivative of the Green function has the physical interpretation of a beam focused to a point, thus eq.(3) is seen to represent the field as a superposition of point-focused beams, weighted by the incident pressure field p(x) on the plane x_3=0.

The problem to be addressed is the transmission of the beam represented by eqs.(1, 3) into a titanium billet. An underlying assumption of the present work is that the billet surface profile geometry is sufficiently well behaved to enable the use of ray theory as a transmission model. Thus any field which is adequately represented by ray theory in the absence of the billet can be adequately represented by applying ray transmission principles in the presence of the billet. The problem faced in this work is that the diffracting beams generated by the transducers of interest are generally not representable by a simple ray theory, hence ray theory is not directly applicable to the problem regardless of the presence of the billet. It was observed, however, that G(x'-x) is quite effectively represented by ray theory. Hence, a solution scheme was developed which is verbally described as representing the incident beam as a superposition of point-focused beams (eq.3), transmitting each beam through the billet surface independently, then summing the transmitted beam components at x' in the billet interior. This concept is expressed

$$\phi(x') = \int_{x_3=0} p(x)\, \bar{G}(x \,|\, x')\, d\underline{x} \tag{5}$$

where the $\bar{G}$ denotes the response of the water/billet system to the point focus beam, i.e., the x_3 derivative of the Green state response of the water/billet system, and ϕ is a displacement potential (transmitted compressional waves are only considered here). Note that the argument of $\bar{G}$ is not convolutional. Algorithmically, eq.(5) is integrated numerically, where $\bar{G}$ is evaluated using a ray theory approximation.

The response $\bar{G}$ is obtained by transmitting the incident field G(x'-x) into the billet via ray theory. For large k_w r, eq.(4) approaches

$$G(x' - x) \approx C \frac{x_3}{r^2} exp(ik_w r) \tag{6}$$

which is recognized as satisfying ray theory eikonal and transport equations.[1] Expressions are needed for ray transmission of eq.(6) through an arbitrarily curved surface. Specifically, an algorithm is required which determines the field phase and amplitude along the ray connecting the point x in the reference plane to the point x' in the billet interior. For the present discussion, the billet surface is parameterized x_3= h(x_1,x_2). For algebraic convenience, non-orthogonal ray coordinates X(s) are defined, where s = (x_1, x_2, l) and l is distance from the surface intersection perpendicular to the phase front. The surface intersection point

$x^1=X(s^1)$ is obtained by an efficient recursive expression (~ 5 iterations to convergence). The field phase at x' is obtained as

$$f(x',x) = |x^i - x|\, k_w + |x' - x^i|\, k_l \tag{7}$$

where k_w and k_l are wavenumbers in the water and solid, respectively. The amplitude A of the transmitted ray is determined by

$$A(x') = A_0(x,x^i)\, T(x,x^i)\, (J(s^i) / J(s))^{1/2} \tag{8}$$

where A_0 is the incident ray amplitude at x^i, T is the plane wave transmission coefficient at x^i for incident orientation x^i - x, and J is the Jacobian of the ray-to-global coordinate mapping.[1] The Jacobian evaluation is a conceptually straightforward but involved task of differential geometry. Details of this analysis or its algorithmic encoding are omitted for brevity.

For the purposes of discussion, eq.(5) is re-written

$$\phi(x') = \int M(x,x')\, exp(\, i\, P(x,x')\,)\, d\underline{x} \tag{9}$$

where M and P are the modulus and phase of the integrand. The reference plane *P* is discretized by an equi-spaced grid of points x^n numbered by a single index n, with separation Δ. Over the patch D_n, defined as $x_j^n - \Delta/2 < x_j < x_j^n + \Delta/2$, j=1, 2, the phase P is written

$$P(x,x') = P(x^n,x') + \partial_j P(x^n,x')\, (x_j - x_j^n) + P_r(x,x',x^n) \quad (sum\ on\ j) \tag{10}$$

which is recognized as the first two terms of a power series expansion plus a remainder P_r. Using eq.(10) in eq.(9) and re-arranging yields

$$\phi(x') = \sum_n \int_{D_n} B_n(x,x')\, exp(\, i\, P(x^n,x') + i\, \partial_j P(x^n,x')\, (x_j - x_j^n)\,)\, d\underline{x} \tag{11}$$

$$B_n(x,x') = M(x,x')\, exp(\, i\, P_r(x,x',x^n)\,) \tag{12}$$

Expanding the $B_n(x,x')$ in power series about the x^n yields

$$\phi(x') = \sum_n \sum_{\alpha\beta} B_{n\alpha\beta}(x')\, Q_{n\alpha\beta}(x') \quad ,\alpha,\beta = 0,1,2\ldots \tag{13}$$

$$Q_{n\alpha\beta}(x') = \frac{1}{\alpha!\,\beta!} \int_{D_n} (x_1 - x_1^n)^\alpha\, (x_2 - x_2^n)^\beta\, exp(\, i\, P(x^n,x') + i\, \partial_j P(x^n,x')\, (x_j - x_j^n)\,)\, d\underline{x} \tag{14}$$

$$B_{n\alpha\beta}(x') = \partial_1^\alpha\, \partial_2^\beta\, B_n(x^n,x') \tag{15}$$

It is noted that eq.(14) is readily evaluated analytically. Numerical efficiency arises from the fact that eq.(12) is a slowly varying function, thus a relatively coarse numerical grid x^n yields acceptable convergence (typically 16x16). In the present implementation, terms to second order are retained in the expansion of $B_n(x,x')$.

Convergence of the quadrature scheme outlined in eqs.(9-15) requires an accurate expansion of $B_n(x,x')$ over the patch D_n. Indeed, the adequacy or existence of such an expansion represents a general statement of the problem to be solved. As previously mentioned, the surface profile is assumed sufficiently well behaved for an efficient expansion. It is convenient, however, to consider discontinuous pressure profiles p(x) over the reference plane, as described by an ideal aperture, which are poorly approximated by global power series expansions. To address this problem, an aperture function is explicitly built into the quadrature scheme. An aperture curve (e.g. a circle) is inscribed within the discretized portion of the reference plane. The points at which the aperture curve intersects the D_n patch boundaries are connected by straight line segments. Those portions of the D_n lying on the side of the line segment to the outer side of the aperture are excluded from the domain of integration (i.e. the aperture is approximated by straight line segments). The integration of eq.(14) over

this modified integration domain is still analytically tractable, albeit yielding a more complicated expression for numerical evaluation.

A discussion to draw contrast between the above-described quadrature and the Gauss-Hermite polynomial expansion as utilized in related work in the ETC program is appropriate. Referring to a generic integral form of eq.(9), the Gauss-Hermite expansion assumes a partial expansion of phase P *about a single point* x^0

$$P(x,x') = P(x^0,x') + \partial_j P(x^0,x')\,(x_j - x_j^0) + .5\,\partial_j^2 P(x^0,x')\,(x_j - x_j^0)^2 + \overline{P}_r(x,x',x^0) \quad (\textit{sum on } j) \tag{16}$$

Eq.(9) is then written

$$\phi(x') = \int_P \overline{B}_0(x,x')\, exp(\, i\, P(x^0,x') + i\,\partial_j P(x^0,x')\,(x_j - x_j^0) + .5\,\partial_j^2 P(x^0,x')\,(x_j - x_j^0)^2\,)\, d\underline{x} \tag{17}$$

$$\overline{B}_0(x,x') = M(x,x')\, exp(\, i\,\overline{P}_r(x,x',x^0)\,) \tag{18}$$

It is seen that terms to second order are retained in the exponential phase factor in eq.(17), and integration is over the the infinite domain P (it is mentioned that the Gauss-Hermite expansion is applied to k-space integrals in the related work of interest: reference to eq.(9) is purely formal). Eq.(18) is likewise expanded about x^0 to yield

$$\phi(x') = \sum_{\alpha\beta} \overline{B}_{0\alpha\beta}(x')\,\overline{Q}_{0\alpha\beta}(x') \quad ,\alpha,\beta = 0,1,2\ldots \tag{19}$$

$$\overline{Q}_{0\alpha\beta}(x') = \frac{1}{\alpha!\,\beta!} \int_P (x_1 - x_1^0)^\alpha\,(x_2 - x_2^0)^\beta$$
$$exp(\, i\, P(x^0,x') + i\,\partial_j P(x^0,x')\,(x_j - x_j^0) + .5\,\partial_j^2 P(x^0,x')\,(x_j - x_j^0)^2\,)\, d\underline{x} \tag{20}$$

$$\overline{B}_{0\alpha\beta}(x') = \partial_1^\alpha\,\partial_2^\beta\,\overline{B}_n(x^0,x') \tag{21}$$

It is noted that the integrals of eq.(20) can be treated analytically, and are represented in terms of Gauss-Hermite Polynomials. It is observed that eq.(19) expresses the field as the sum of integrals with quadratic phase dependence in the integrand, whereas eq.(13) expresses the field as the sum of integrals with a piece-wise linear phase dependence in the integrand. The preference for one representation over the other would appear to depend on the behavior of the integrand. In cases where in eq.(9) the phase is nearly quadratic and the modulus is sufficiently smooth, the Gauss-Hermite representation is extremely efficient. It is often the case, however, that it is more efficient to represent a function over a distributed grid of points rather than in an expansion about a single point, particularly if the function displays complicated behaviors. Indeed, it is easy to concoct simple problems for which the expansions of eqs.(16-21) do not exist.

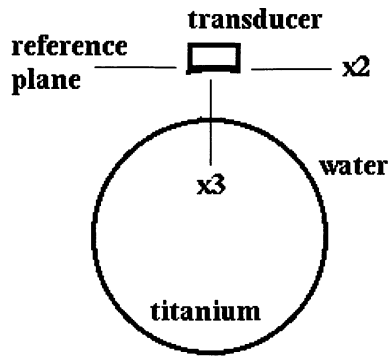

Fig. 1 Transducer-billet configuration.

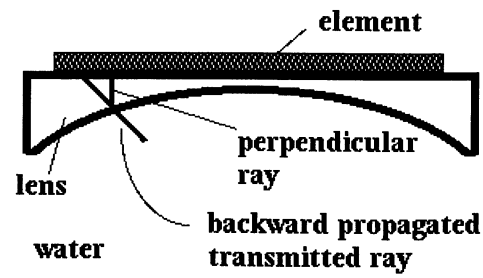

Fig. 2 Bi-cylindrical lens grometry.

Use of the beam model presented in the preceding section requires the prescription of an incident pressure field distribution on the reference plane in the fluid medium. A model for the prescription of a pressure field as generated by a bi-cylindrically focused lens/fixed element system is discussed, based on an elementary application of ray theory. It is argued that this treatment is appropriate since propagation over a very short distance is being considered. The lens geometry is depicted in fig.2. The reference plane P is chosen as the lens-element interface. Propagation from the circular transducer element to the lens surface is modeled by rays emerging perpendicular to the element originating at points on a rectangular grid on the reference plane. These rays are refracted through the lens element according to Snell's law, and the field amplitude along these rays is reduced according to angular-dependent plane wave transmission coefficients. Variations in lens material velocity and attenuation are also allowed in the formulation. Following transmission, the rays are backward-traced to the reference plane as if the lens were absent. The algorithm then interpolates this reference plane pressure onto a regular spaced grid for future use. This process can be viewed as having the beam originate at the "virtual" reference plane seen looking backward through the lens. This approach initiates aperture diffraction closer to the actual propagation path distance, as opposed to, say, initiating aperture diffraction at some reference plane forward of the lens. The model is seen to treat only diffraction at the element edge (more accurately, the "virtual element" edge). Diffraction at the lens edges is ignored, as if the lens were considerably larger than the element. Multiple reflections within the lens are likewise ignored.

NUMERICAL RESULTS

Examples of application are now presented. The test case considered is transmission into a 10 inch diameter titanium billet. The worst-case test of focusing to the billet center is studied. The first example compares focal zone geometries for two different diameter transducer elements. Using geometric optics formulae, the bi-cylindrical lens radii are specified to focus at the center of the billet using a 3 inch water path, resulting in r_1=12.15, r_2 = 3.96, where r_1 and r_2 are the lens radius in the x_1 , x_2 directions in inches, respectively. Fig.3 compares the amplitude profiles down the central axis of the beam for element diameters of 2.35 and 4.0 inches. With the 2.35 in. dia. element, focusing occurs short of the intended geometric focus by 0.32 inches due to aperture diffraction. The larger 4.0 inch aperture is seen to significantly reduce the error in the intended focal depth, falling short of the intended focus by only .025 inches. It is mentioned that the curves in fig.3 are normalized to a maximum amplitude of unity. The peak field amplitude generated by the 4.0 in. aperture is a factor of 2.3 larger than the 2.35 in. aperture, due to the combined effects of greater focusing and greater total element energy output. Note that the larger aperture produces a focal zone with a more complicated geometric structure, due to a more pronounced phase interference pattern, and that the depth of field is considerably less. The pronounced interference minima seen in viewing time harmonic results will, of course, be less pronounced when considering broadband time-dependent pressure amplitude distributions. The focal zone prediction capability demonstrated in fig.3 is being used in the ETC program to aid in the design and procurement of transducers. In practice, the transducer element size is limited to less than ~ 2.35 in. dia., due to physical limitations in fabrication and piezoelectric response. Therefore, model simulations are being used to adjust the lens radii to obtain focusing at desired depths.

Results are presented which demonstrate the effect of surface irregularity on the focal zone geometry. It is instructive to note that the bi-cylindrical lens and billet surface work together to form a compound element focusing system. It is well understood that machining tolerances to within a fraction of a wavelength must be maintained if the bi-cylindrical lens surface is to function properly. Equally important, however, is the precision of the machining of the second focusing element: the billet surface. Indeed, the geometric precision of

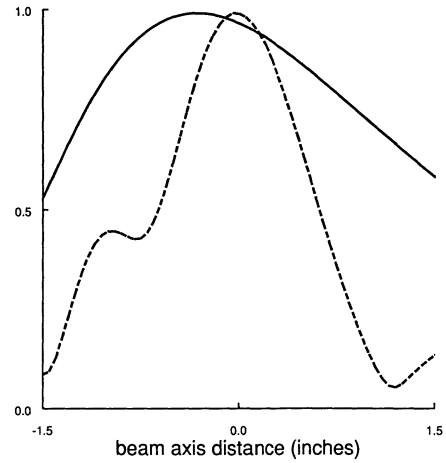

Fig. 3 Axial beam profiles for (——) 2.35 and (- - -) 4.0 in. dia. apertures.

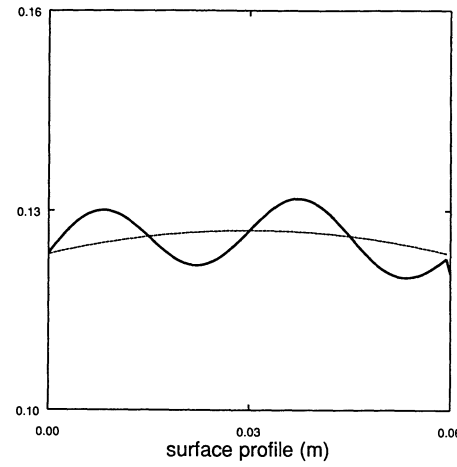

Fig. 4 Sinusoidal surface wander added to circular billet profile.

the billet surface is actually more critical, due to the larger velocity mismatch between water and titanium. Practically speaking, the billet surface will be machined nowhere near the tolerances required for focusing performance as predicted in the above model simulation. Therefore, the model simulation is used to examine the sensitivity to surface irregularities to be expected. The surface irregularities of most concern are not necessarily surface roughness, but rather surface wandering which might tend to put a large fraction of the beam footprint significantly out of phase with that required for an accurate focus. As an example, the circular cylindrical surface profile considered in fig.3 is modified by adding a sinusoidal perturbation with a period of 3 cm. This period was chosen so that approximately one period of the sinusoidal profile would fit within the beam footprint on the surface. An extremely exaggerated profile modification is shown in fig. 4 to facilitate description. Calculations were performed using profile heights of 0.1 and 0.2 mm, which are barely perceptible if plotted in similar fashion to fig. 4. Transducer parameters were taken as those in fig. 3. Fig. 5 shows the corresponding changes in the beam profile along the beam central axis. Fig. 6 shows the effect on the beam profile taken perpendicular to the central beam axis, in the radial direction through the center of the billet (x_2 direction in fig.1). A significant redistribution of energy is seen to result from the phase perturbations at the beam footprint introduced by the sinusoidal surface irregularity. It is mentioned that this is not a special consequence of choosing a sinusoid for a profile modification - any modification having bumps of approximately the same size and height would introduce similar effects on the focus. These results indicate the importance of surface wander as an issue, and raises this as a topic of concern to POD estimation in billet inspection.

Finally, results are presented to compare with predictions of a Gauss-Hermite polynomial expansion beam model. This model is based on a Gauss-Hermite polynomial expansion of Fourier transform integrals such as eq.(1), in which the effective width of the beam spatial frequency spectra are modified according to the local radii of curvature of the surface at the surface intersection point of the incident beam central axis.[2] Results of figs. 5 and 6 for h=0 are compared with Gauss-Hermite model predictions in fig. 7. Note that the two results show good agreement, thus establishing confidence in model POD predictions in related ETC program work employing the Gauss-Hermite model. Note, however, in the sinusoidally perturbed surface profile results of figs. 5 and 6, the radii of surface curvature at the beam central axis surface intersection is the same for all three cases shown. Therefore the Gauss-Hermite model would have predicted the results of fig. 7 for all three cases. This fact is not necessarily due to an inherent limitation in the applicability of the

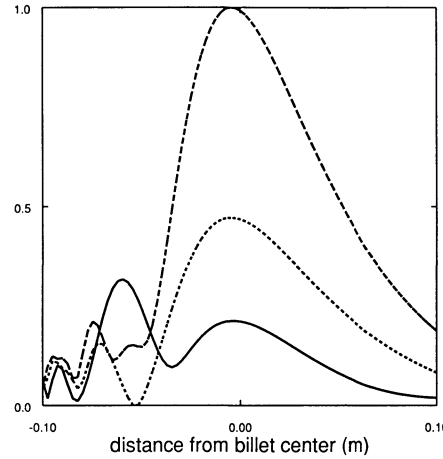

Fig. 5 Axial beam profiles for varying surface height h in fig. 4.
(– – –) h = 0.0 mm, (- - -) h = 0.1 mm, (——) h = 0.2 mm.

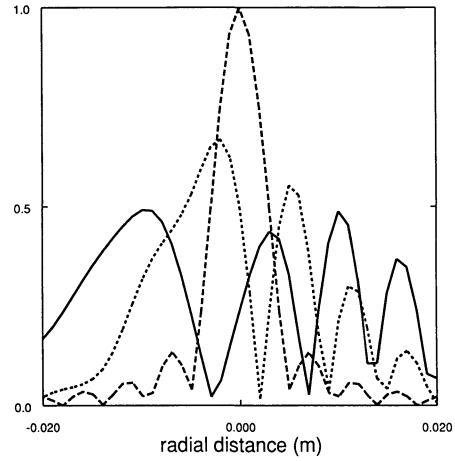

Fig. 6 Lateral beam profiles (radial billet direction) for varying surface height h in fig. 4.
(– – –) h = 0.0 mm, (- - -) h = 0.1 mm, (——) h = 0.2 mm.

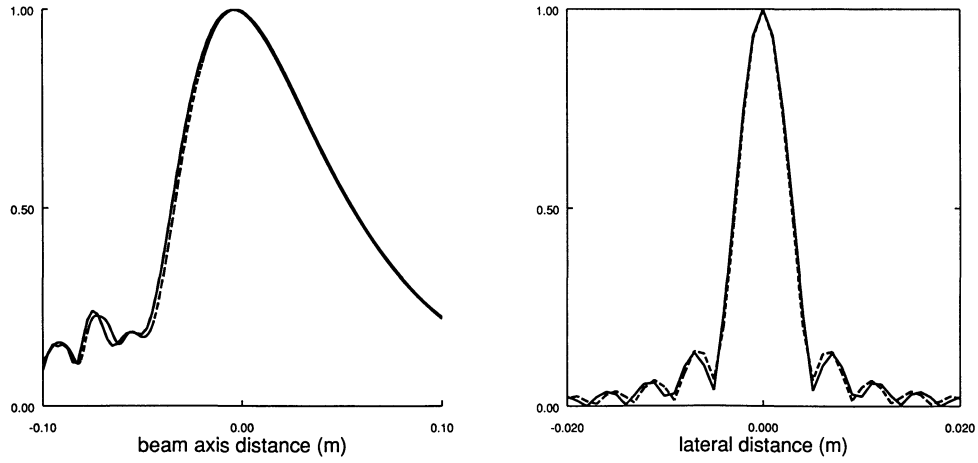

Fig. 7 Comparison with Gauss-Hermite model predictions; a) axial b) lateral beam profiles.
(– – –) Gauss-Hermite model, (——) results of figs.5,6 with h=0.

Gauss-Hermite expansion, but rather to the limited expansion used in constructing the specific algorithm considered here. More sophisticated Gauss-Hermite expansion-based algorithms are under development, and performance comparisons are planned for the future.

SUMMARY

This paper discussed a beam propagation model being employed to study beam focusing phenomena of interest in titanium billet inspection work being performed by the FAA ETC program. The model is based on a Green function- boundary integral problem formulation, in which the Green function is the point response for the water-billet system. The Green function is evaluated using high-frequency asymptotics (ray theory), and the boundary integral is numerically evaluated using an efficient, novel quadrature which analytically treats aperture edge diffraction. Focusing by a bi-cylindrical lens is studied using a simple ray theory model to generate fluid pressure fields as would be generated by the lens for use in the beam transmission algorithm. Examples were discussed which demonstrate the dependence of the focal zone geometry on aperture radius and billet surface geometry.

ACKNOWLEDGMENT

This work supported by the FAA Engine Titanium Consortium program.

REFERENCES

1. J.D. Achenbach, A.K. Gautesen, H. McMaken, *Ray Methods for Waves in Elastic Solids,* Pitman, 1982.
2. R.B. Thompson, T.A. Gray, J.H. Rose, V.G. Kogan, E.F. Lopes, "The Radiation of Elliptically and Bi-Cylindrically Focused Piston Radiators," J. Acoust. Soc. Amer. 82, p.1818, 1987.